

(Y,Gd)BO₃:Eu red phosphor for dual-layer phosphor structure to enhance the optical performance of white light-emitting diodes

Phan Xuan Le, Le Hung Tien

Faculty of Engineering, Van Lang University, Viet Nam

Article Info

Article history:

Received Feb 24, 2021

Revised Apr 26, 2021

Accepted May 25, 2021

Keywords:

(Y,Gd)BO₃:Eu
Color quality scale
Luminous efficacy
White LED

ABSTRACT

Among the structures using for fabricating white light-emitting diodes (WLEDs) such as the conformal coating or in-cup geometries, the remote phosphor structure gives the highest luminous efficacy. However, in terms of color quality, its performance is not as good as the others. The red-light compensation has been reported as the effective solution for enhancing the color quality of WLEDs. Hence, this study adopted the idea and applied to the dual-layer phosphor structure. The phosphor used to boost the red color in light formation is (Y,Gd)BO₃:Eu particle. The dual-layer remote phosphor structure was simulated with the red (Y,Gd)BO₃:Eu phosphor layer above the original yellow phosphor YAG:Ce³⁺ one. The WLEDs with different correlated color temperatures of 5600 K, 6600 K and 7700K were experimented. Mie-theory and Lambert-Beer law were applied to examine the results. The growth in color rendering index (CRI) and color quality scale (CQS) with the increase of (Y,Gd)BO₃:Eu phosphor concentration was observed. Nevertheless, the lumen efficacy would be degraded if the concentration was over a certain number. The information provided in this article is useful for the development of high-power WLED production with greater color quality.

This is an open access article under the [CC BY-SA](https://creativecommons.org/licenses/by-sa/4.0/) license.



Corresponding Author:

Phan Xuan Le
Faculty of Engineering,
Van Lang University,
No. 45 Nguyen Khac Nhu Street, Ho Chi Minh City, Vietnam
Email: le.px@vlu.edu.vn

1. INTRODUCTION

We have witnessed a fast development of solid-state lighting (SSL) technology in the lighting market and industry over the past few years. It presents a high level of lighting efficiency and eco-friendliness. The phosphor-converted white light-emitting diode (pc-WLED) has been emerged as a competitive candidate for SSL to replace the traditional lighting sources, for instances, the incandescent and fluorescent lamps [1]-[3]. As the pc-WLEDs own unique features, not only high efficiency and safety but also high stability and robustness, they have been widely applied in indoor and outdoor uses, for example, backlighting, or residential, industrial and commercial lightings. However, the pc-WLED usually struggles with its inefficient light extraction and the non-uniform angular-correlated color temperature (CCT) [4], [5]. Thus, it is essential to increase the chromatic uniformity and lumen efficiency of WLED devices for them to be able to catch up with rising demands of the market [6]-[8]. Usually, a pc-WLED is fabricated with a blue LED chip and a phosphor layer of yellow YAG:Ce³⁺ particles. The white light is generated from the mixture of blue lights excited by the blue chip and yellow lights emitted from YAG:Ce³⁺ phosphor film.

Therefore, the optical performance of the WLED significantly relies on the properties of the YAG:Ce³⁺. In addition to that, the organization of the components inside the WLED is another vital feature that greatly influences the efficiency of light extraction and color adequacy [9]-[12]. There have been many methods applied to adjust the arrangement of the phosphor film and the blue chip of a LED. Amongst those, the phosphor coating techniques are the most commonly used, for example dispensing coating and conformal coating, as they can give good color quality. Yet, the luminescence of the pc-WLEDs with these geometries does not high or even declines owing to the light conversion reduction of the phosphor. Such degradation is primarily caused by the heat increase at the phosphor-LED chip interface, since using these coating methods means that the phosphor material directly contacts with the LED chip (heat source). To protect the phosphor material from the heat damage and improve the luminous flux while achieving high color homogeneity for WLEDs, it is important to separate the phosphors from the LED chip. Hence, previous studies had proposed a promising structure adopting this idea, which is the remote phosphor structure [13]-[16].

By creating an appropriate distance between the phosphor and the LED chip, this structure could minimize not only the heat effect but also the series of light backscattering inside the WLED package, thus the luminous efficiency can be enhanced significantly [17], [18]. However, the original remote phosphor structure is suitable for general lighting devices, not for other state-of-the-art lighting applications. Thus, the investigation in developing remote phosphor structure is needed. Some advances had been made in the fabrication of the remote phosphor structures to limit the backscattered lights for better lumen output. A structure of a ring remote phosphor layer that surrounds an inverted cone lens encapsulant was proposed. This structure did enhance the lumen output as it can direct the lights excited from the chip straight to the LED surface, which greatly reduced the amounts of lights lost from the light reflection inside the WLED package [19]-[21]. Another study reported the ability of yielding high angular CCT uniformity and stability of a patterned remote phosphor structure having the surrounding area uncoated with phosphors [22]. Additionally, the patterned sapphire substrate used in the remote phosphor structure was demonstrated to have better color uniformity in the far field pattern than in the near one [23]. However, in these reports, it seems impossible for the remote phosphor structure to achieve high chromatic homogeneity and adequate luminous efficiency at the same time.

In this study, we suggested using a remote phosphor structure with an additional phosphor layer placed above the yellow YAG:Ce³⁺ phosphor film. This dual-layer remote phosphor structure is believed to yield higher color quality and lumen efficiency simultaneously. The additional phosphor layer in our study uses red phosphor (Y,Gd)BO₃:Eu particles to boost the red light components, leading to more homogenous generated white lights. The effects of the two phosphor layers on the color quality were examined via two parameters: color rendering index (CRI) and color quality scale (CQS). In addition, the photoluminescence of the dual-layer remote structure was investigated and demonstrated. The contents of this study are organized as; section 2 is used for demonstrating the process of preparing the phosphor material and the simulation of the dual-layer remote phosphor WLED package. Next, the results obtained from experiments are presented and explained in section 3. Section 4 is the summary and conclusion of the research.

2. COMPUTATIONAL SIMULATION

2.1. Phosphor preparation

The preparation of the red (Y,Gd)BO₃:Eu phosphors is the first important step in the process of WLED simulation. Table 1 showed the chemical composition of (Y,Gd)BO₃:Eu in which the details of ingredients with their corresponding mole percentage and weight were clearly demonstrated. The (Y,Gd)BO₃:Eu preparation process includes four stages. The first stage is well-mixing all the ingredients by dry blending. Then, the mixture goes through two continuous firing stages. In the first time, it is fired in capped quartz tubes or in alumina crucibles with air, and at the temperature range of 400°C-500°C. The next firing is carried out under the same condition with the first one but at the higher temperature, 1100°C. After that, the mixture is taken out and powderized. Then, the powder is slurried in boiling HCl of 10% for 30 minutes. Next, the slurry is washed with boiling water and decanted. This washing step should be repeated until the product is neutral. Then, drying the product in air, at the temperature of 110°C. When the products are dried, we will get the red phosphor (Y,Gd)BO₃:Eu needed for experiments. The red phosphor adequate for the experiments have the emission color of red and the highest emission at 619 nm.

Table 1. Chemical composition of red-emitting phosphor (Y,Gd)BO₃:Eu

Ingredient	Mole %	by Weight (g)
Y ₂ O ₃	32	72.2
Gd ₂ O ₃	15	54.4
Eu ₂ O ₃	3	10.6
H ₃ BO ₃	130	80.4

2.2. Constructing the WLEDs configuration

The simulation of a WLED package with a dual-layer remote phosphor structure was carried out using the LightTools 9.0 program and Mie-scattering theory. Moreover, with the application of Mie theory, the analysis on the effect of the dual-layer phosphor package on the optical properties of WLEDs with CCTs from 5600 K to 7700 K is easily conducted. The in-cup phosphor configuration with the dual-layer remote phosphor was presented in Figure 1. As can be seen, the arrangement of phosphor layers are as the following: red phosphor $(Y,Gd)BO_3:Eu$ layer, the yellow $YAG:Ce^{3+}$ film and the silicone glue.

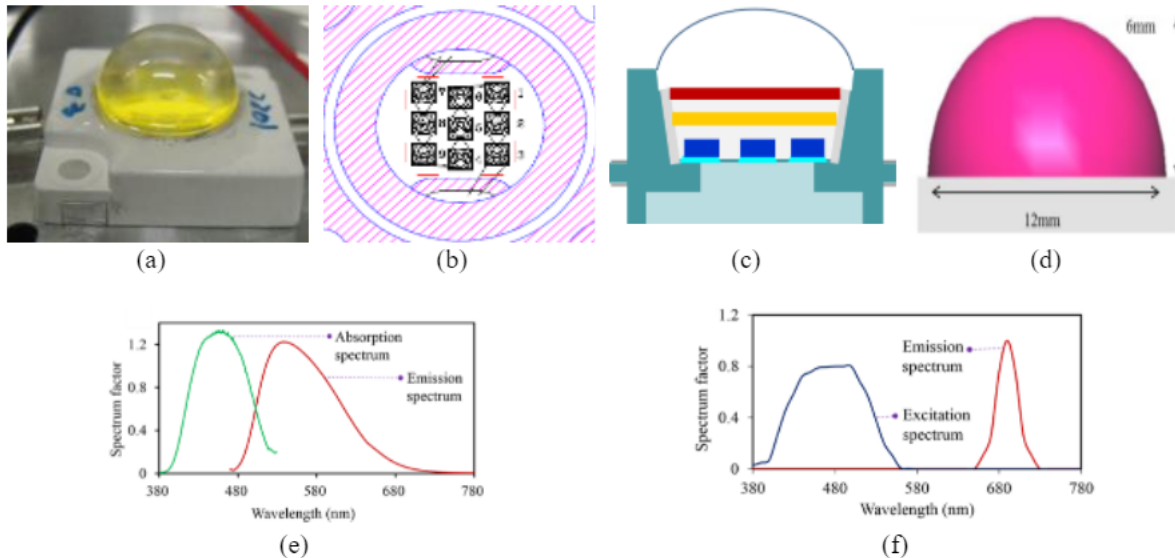


Figure 1. Photograph of WLEDs structure; (a) actual WLEDs, (b) bonding diagram, (c) illustration of pc-WLEDs model, (d) simulation of WLEDs using lighttools commercial software, (e) the measured spectra of the yellow-emitting $YAG:Ce$ phosphor, (f) the measured spectra of the red-emitting $(Y,Gd)BO_3:Eu$ phosphor

The other elements of the WLED simulation includes blue LED chips and a reflector cup. It is noted that the number of chips used in this study is nine. Each blue chip has a radiant power of 1.16 W and a peak wavelength of 453 nm. For the reflector, which is bonded with the blue chips, the lengths at the top and bottom surfaces are 8 mm and 9.85 mm, respectively, while its depth is 2.07 mm. An crucial point in using the additional layer of red phosphor $(Y,Gd):BO_3:Eu$ is that the yellow phosphor $YAG:Ce^{3+}$ concentration must be adjusted following the change in $(Y,Gd):BO_3:Eu$ concentration to keep the CCT stable. This relation was clearly displayed in Figure 2. There are two notions that can be realized from this yellow-phosphor concentration adjustment. Firstly, it is to maintain the CCT of the WLED package; and secondly, it probably has significant effects on the light scattering and light absorption inside the WLEDs, leading to the changes in yielded color quality and lumen output. The use of red phosphor layer is to achieved better color uniformity for the remote phosphor structure, yet the lumen output must be monitored to fulfill the goal of the study.

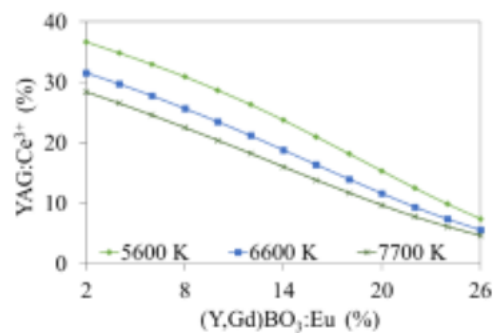


Figure 2. The change of phosphor concentration for keeping the average CCTs

3. RESULTS AND DISCUSSION

The color quality of the a WLED is usually evaluated with color rendering index (CRI), thus we carried out the investigation on the CRI of the WLED structure with different concentrations of (Y,Gd)BO₃:Eu phosphor, as shown in Figure 3. The rise in CRI was observed as the (Y,Gd)BO₃:Eu amount increased, due to the stronger red-light emission. Additionally, the weight percentage of (Y,Gd)BO₃:Eu phosphor from 0% to 24% is in direct proportion to the CRI. In other words, when the (Y,Gd)BO₃:Eu weight percentage grew from 0% to 24%, the CRI also increased. Especially, the CRI over 86 was observed at about 24% wt. (Y,Gd)BO₃:Eu. However, if the concentration of (Y,Gd)BO₃:Eu exceeded 24% wt., the CRI would decline owing to the excessive red-light proportion. In the market, the WLED devices having higher CRI probably cost more than the rest ones. A benefit of using the red phosphor (Y,Gd)BO₃:Eu in fabricating dual-layer remote phosphor WLED is its low cost. Thus, this red phosphor is practical for WLED manufacturers. Since the WLED color quality evaluation is comprised of several factors and one of them is CRI, it is impossible to use only the CRI to examine the chromatic performance of white lights. Another parameter which is believed to be more powerful in evaluating the color homogeneity of WLED was proposed in recent studies. This is the color quality scale (CQS). CQS can help the white-light color evaluation to be more accurate because it is comprised of CRI and two other factors: viewer's preference and color coordinates.

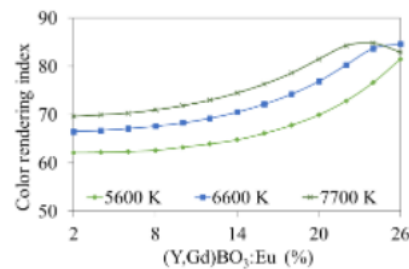


Figure 3. The color rendering index of WLEDs as a function of (Y,Gd)BO₃:Eu concentration

Figure 4 demonstrated the CQS of three WLED models with three different CCTs when using the additional red phosphor layer. Obviously, the red phosphor (Y,Gd)BO₃:Eu is suitable for increasing the color quality as the CQS values enhanced in connection with the rise of its concentration. Thus, the study has achieved the first goal of enhancing the color quality for WLED with remote phosphor structure by utilizing the red-emitting phosphor (Y,Gd)BO₃:Eu. However, the disadvantages it causes to the luminous flux should not be ignored. As can be seen in Figure 5, the luminous flux of WLED tended to decrease when we increased the red phosphor concentration, at all CCTs. The degradation in lumen efficiency can be explained by the scattering effects of (Y,Gd)BO₃:Eu phosphors via Mie-theory.

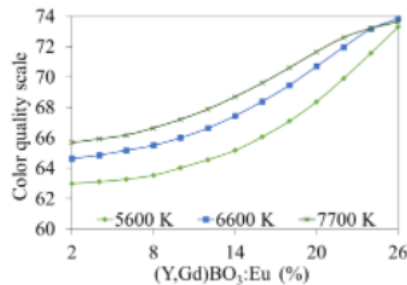


Figure 4. The color quality scale of WLEDs as a function of (Y,Gd)BO₃:Eu concentration

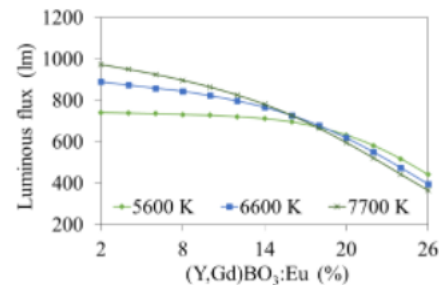


Figure 5. The lumen output of WLEDs as a function of (Y,Gd)BO₃:Eu concentration

Mie-scattering theory [24], [25] was also a useful mean in computing scattering cross section C_{sca} for phosphor particles with the spherical shape. In addition to that, Lambert-Beer law was utilized to compute the power of transmitted lights:

$$I = I_0 \exp(-\mu_{ext}L) \quad (1)$$

Here, I_0 , L , and μ_{ext} present the incident light power, the thickness of the phosphor layer (mm), and the extinction coefficient, respectively. The μ_{ext} can be computed via this expression: $\mu_{ext} = N_r \cdot C_{ext}$, in which N_r (mm^{-3}) indicates the particles' number density distribution, and C_{ext} (mm^2) shows the phosphor particles' extinction cross-section. Based on (1), the increase of phosphor concentration got the internal light scattering developed and caused the degradation in light transmission efficiency. However, from the values presented in Figure 5, we can maintain the luminous flux at high value if the concentration of $(\text{Y,Gd})\text{BO}_3:\text{Eu}$ stays below 14%. At that concentration level the CRI and CQS of the WLED were also improved, compared to the structures without $(\text{Y,Gd})\text{BO}_3:\text{Eu}$ (0% wt.), see Figure 3 and Figure 4. It is depended on the goals of manufacturers, the concentration of $(\text{Y,Gd})\text{BO}_3:\text{Eu}$ is decided. A small reduction in lumen output is unavoidable if they want to produce WLEDs with high color quality.

In general, the white light is generated via the combination of three different spectral regions, as displayed in Figures 6-8. Obviously, the red spectral region (648 nm-738 nm) presented significant enhancement as the $(\text{Y,Gd})\text{BO}_3:\text{Eu}$ concentration increased. This can be observed in three WLED models having CCTs of 5600 K, 6600 K and 7700 K, respectively. Moreover, the rise in other two spectral regions, 420-480 nm and 500-640 nm, contributed remarkably to the red one. The enhancement in these two spectral zones promoted the blue-light scattering. Besides, the emission spectra were higher when the CCT is higher, leading to the better color and luminous performances. This result reinforced the idea of using $(\text{Y,Gd})\text{BO}_3:\text{Eu}$ red phosphor to improve to optical properties of the WLED remote phosphor structure. This is also important and useful for manufacturers when achieving the control over the color quality of WLEDs, especially the ones with high CCT such as 7700 K, is still difficult for remote phosphor structure.

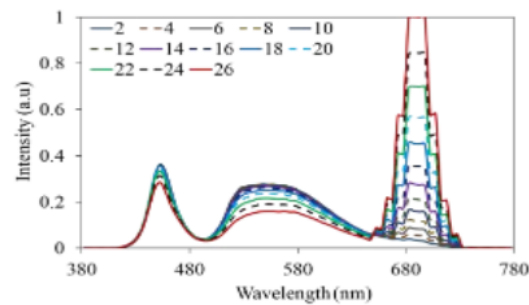


Figure 6. The emission spectra of 5600K WLEDs as a function of $(\text{Y,Gd})\text{BO}_3:\text{Eu}$ concentration

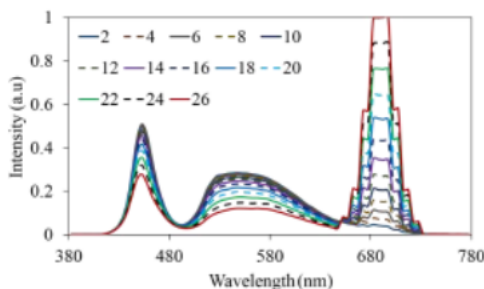


Figure 7. The emission spectra of 6600 K WLEDs as a function of $(\text{Y,Gd})\text{BO}_3:\text{Eu}$ concentration

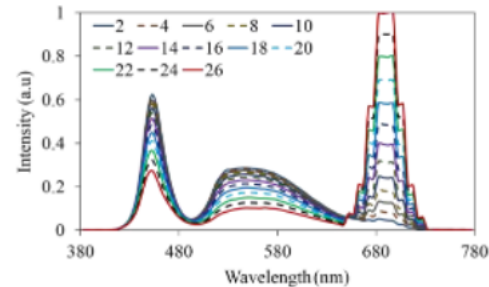


Figure 8. The emission spectra of 7700 K WLEDs as a function of $(\text{Y,Gd})\text{BO}_3:\text{Eu}$ concentration

4. CONCLUSION

The influences of $(\text{Y,Gd})\text{BO}_3:\text{Eu}$ red phosphor on the color quality and luminous efficiency of WLED with dual-layer remote phosphor configuration were presented in this research paper. By applying Mie theory and Beer's law, the results were examined and verified. The benefits of using $(\text{Y,Gd})\text{BO}_3:\text{Eu}$ red phosphors in heightening the color quality for remote phosphor structure were recognized through the enhancement of both CRI and CQS. This can be applicable to WLED with low CCT (e.g. 5600 K) and high CCT (e.g. 7700 K). Meanwhile, the luminous efficacy still presented a reduction if the red phosphor concentration exceeded 14% wt. The manufacturers are the ones that decide the suitable phosphor concentration to accomplish their goals. If they want a WLED product using remote phosphor structure and

able to yield high color quality and lumen efficacy at the same time, they can select the (Y,Gd)BO₃:Eu concentration at around 14% wt.

REFERENCES

- [1] S. Kashima, *et al.*, "Wide field-of-view crossed Dragone optical system using anamorphic aspherical surfaces," *Appl. Opt.*, vol. 57, no. 15, pp. 4171-4179, 2018, doi: 10.1364/AO.57.004171.
- [2] T. Han, *et al.*, "Spectral broadening of a single Ce³⁺-doped garnet by chemical unit cosubstitution for near ultraviolet LED," *Opt. Mater. Express*, vol. 8, no. 12, pp. 3761-3769, 2018, doi: 10.1364/OME.8.003761.
- [3] X. Liu, *et al.*, "Upconversion luminescence, intrinsic optical bistability, and optical thermometry in Ho³⁺/Yb³⁺:BaMoO₄ phosphors," *Chin. Opt. Lett.*, vol. 17, no. 11, pp. 111601-, 2019.
- [4] Wang, *et al.*, "Eu³⁺ doped high-brightness fluorophosphate laser-driven glass phosphors," *Opt. Mater. Express*, vol. 9, pp. 1749-1762, 2019.
- [5] S. Kim, *et al.*, "High-speed color three-dimensional measurement based on parallel confocal detection with a focus tunable lens," *Opt. Express*, vol. 27, pp. 28466-28479, 2019.
- [6] W. Gao, *et al.*, "Color temperature tunable phosphor-coated white LEDs with excellent photometric and colorimetric performances," *Opt. Express*, vol. 57, pp. 9322-9327, 2018.
- [7] N. Rashid, *et al.*, "Spectrophotometer with enhanced sensitivity for uric acid detection," *Chin. Opt. Lett.*, vol. 17, no. 8, pp. 081701-, 2019.
- [8] Y. Zhang, *et al.*, "Modeling and optimizing the chromatic holographic waveguide display system," *Appl. Opt.*, vol. 58, no. 34, pp. G84-G90, 2019, doi: 10.1364/AO.58.000G84.
- [9] T. Ya. Orudzhev, S. G. Abdullaeva and R. B. Dzhabbarov, "Increasing the extraction efficiency of a light-emitting diode using a pyramid-like phosphor layer," *J. Opt. Technol.*, vol. 86, no. 10, pp. 671-676, 2019, doi: 10.1364/JOT.86.000671.
- [10] Leipeng Li, Yuan Zhou, Feng Qin, Yangdong Zheng and Zhiguo Zhang, "On the Er³⁺ NIR photoluminescence at 800 nm," *Opt. Express*, vol. 28, no. 3, pp. 3995-4000, 2020, doi: 10.1364/OE.386792.
- [11] R. A. Deshpande, A. S. Roberts and S. I. Bozhevolnyi, "Plasmonic color printing based on third-order gap surface plasmons [Invited]," *Opt. Mater. Express*, vol. 9, no. 2, pp. 717-730, 2019, doi: 10.1364/OME.9.000717.
- [12] Ahmad, *et al.*, "Characterization of color cross-talk of CCD detectors and its influence in multispectral quantitative phase imaging," *Opt. Express*, vol. 27, no. 4, pp. 4572-4589, 2019, doi: 10.1364/OE.27.004572.
- [13] R. Wan, *et al.*, "Simultaneously improve the luminous efficiency and color-rendering index of GaN-based white-light-emitting diodes using metal localized surface plasmon resonance," *Opt. Lett.*, vol. 44, no. 17, pp. 4155-4158, 2019, doi: 10.1364/OL.44.004155.
- [14] Jingkun Zhou and Keyuan Qian, "Low-voltage wide-field-of-view lidar scanning system based on a MEMS mirror," *Appl. Opt.*, vol. 58, no. 5, pp. A283-A290, 2019, doi: 10.1364/AO.58.00A283.
- [15] H. Chen, *et al.*, "Quadrichromatic LED based mobile phone camera visible light communication," *Opt. Express*, vol. 26, no. 13, pp. 17132-17144, 2018, doi: 10.1364/OE.26.017132.
- [16] T. Kozacki, M. Chlipala, and Hyon-Gon Choo, "Fourier rainbow holography," *Opt. Express*, vol. 26, no. 19, pp. 25086-25097, 2018, doi: 10.1364/OE.26.025086.
- [17] S. W. Jeon, *et al.*, "Optical design of dental light using a remote phosphor light-emitting diode package for improving illumination uniformity," *Appl. Opt.*, vol. 57, no. 21, pp. 5998-6003, 2018, doi: 10.1364/AO.57.005998.
- [18] T. R. Dastidar and R. Ethirajan, "Whole slide imaging system using deep learning-based automated focusing," *Biomed. Opt. Express*, vol. 11, no. 1, pp. 480-491, 2020, doi: 10.1364/BOE.379780.
- [19] J. Chen, *et al.*, "Microlens arrays with adjustable aspect ratio fabricated by electrowetting and their application to correlated color temperature tunable light-emitting diodes," *Opt. Express*, vol. 27, no. 4, pp. A25-A38, 2019, doi: 10.1364/OE.27.000A25.
- [20] Jong-Hoon Kim, Bu-Yong Kim, and Heesun Yang, "Synthesis of Mn-doped CuGaS₂ quantum dots and their application as single downconverters for high-color rendering solid-state lighting devices," *Opt. Mater. Express*, vol. 8, no. 2, pp. 221-230, 2018, doi: 10.1364/OME.8.000221.
- [21] S. Sadeghi, *et al.*, "Quantum dot white LEDs with high luminous efficiency," *Optica*, vol. 5, no. 7, pp. 793-802, 2018, doi: 10.1364/OPTICA.5.000793.
- [22] A. Neitz, *et al.*, "Effect of cone spectral topography on chromatic detection sensitivity," *J. Opt. Soc. Am. A*, vol. 37, no. 4, pp. A244-A254, 2020, doi: 10.1364/JOSAA.382384.
- [23] X. Bao, X. Gu, and W. Zhang, "User-centric quality of experience optimized resource allocation algorithm in VLC network with multi-color LED," *Opt. Express*, vol. 26, no. 21, pp. 27826-27841, 2018, doi: 10.1364/OE.26.027826.
- [24] J. Cheng, *et al.*, "Luminescence and energy transfer properties of color-tunable Sr₄La₂PO₄:Ce³⁺,Tb³⁺,Mn²⁺ phosphors for WLEDs," *Opt. Mater. Express*, vol. 8, no. 7, pp. 1850-1862, 2018, doi: 10.1364/OME.8.001850.
- [25] X. Li, B. Hussain, L. Wang, J. Jiang and C. P. Yue, "Design of a 2.2-mW 24-Mb/s CMOS VLC Receiver SoC With Ambient Light Rejection and Post-Equalization for Li-Fi Applications," in *Journal of Lightwave Technology*, vol. 36, no. 12, pp. 2366-2375, 2018, doi: 10.1109/JLT.2018.2813302.

